Comput Visual Sci 3: 47–59 (2000)

Computing and
Visualization in Science

Regular article

Large Eddy Simulation and the variational multiscale method

Thomas J.R. Hughes[1,*], **Luca Mazzei**[1,**], **Kenneth E. Jansen**[2,***]

[1] Division of Mechanics and Computation, W.F. Durand Building, Stanford University, Stanford, California 94305-4040, USA
[2] Department of Mechanical Engineering, 2044 Jonsson Engineering Center, Rensselaer Polytechnic Institute, Troy, NY 12181, USA

Received 3 June 1999 / Accepted: 20 September 1999

Abstract. A Large Eddy Simulation (LES) formulation is developed from the variational multiscale method. Modeling is confined to the effect of a small-scale Reynolds stress, in contrast with classical LES in which the entire subgrid-scale stress is modeled. All other effects are accounted for exactly. It is argued that many shortcomings of the classical LES/constant-coefficient Smagorinsky model are eliminated by the scale separation inherent *ab initio* in the present approach.

1 Introduction

The variational multiscale method was originally introduced to help elucidate the origins of stabilized finite element methods and provide a variational framework for subgrid-scale modeling, amongst other things (see Hughes [20]). Subsequent developments have been primarily focused on numerical analysis issues, such as equivalence results with residual-free bubbles (Brezzi et al. [2]), time-dependent problems (Hughes and Stewart [22]), and *a priori* error estimation (Brezzi et al. [4, 5]). For a compendium of state-of-the-art contributions to the theory of stabilized methods, residual-free bubbles and multiscale methods, see Franca [13]. In Hughes et al. [21] the multiscale approach is suggested as a paradigm for *a posteriori* error estimation, and the role of "jump" terms on element interfaces is explored. Another recent work of note is that of Guermond [17] in which the idea of artificial diffusion is resuscitated within the context of the multiscale approach and shown to be capable of achieving *a priori* error estimates similar to stabilized methods. This is in contrast to the usual low order of accuracy obtained for classical artificial diffusion methods. A version of this approach in which the diffusivity is identified adaptively is proposed in Brezzi et al. [3]. We may note that the above works emphasize linear model equations, such as the advection-diffusion and Helmholtz equations.

In this work we return to one of our original goals, namely, developing a variational framework for subgrid-scale modeling. Here we consider the application of the multiscale method to the incompressible, isothermal, Navier-Stokes equations. Our objective is a satisfactory interpretation/generalization of the Large Eddy Simulation (LES) concept within a variational formulation of the Navier–Stokes equations. This forces us to deal with nonlinearities as well as issues of turbulence modeling. We view this paper as providing the first step in examining these issues within the multiscale method.

We begin by reviewing the classical LES formulation of the incompressible Navier–Stokes equations. As a point of reference, we discuss filtering, the subgrid-scale stress and the Smagorinsky model. The estimation of Smagorinsky parameters by way of the approach due to Lilly [28–30] is also recalled. We summarize the shortcomings of the classical approach, noted previously in the literature, and review some recent attempts at employing a particular industrial finite element CFD program for LES. These set the stage for the current developments.

We note in passing that a fundamental problem of the classical approach seems to be scale separation. The way this problem has been addressed in recent years is by way of dynamic modeling, which provides for adaptive selection of the so-called Smagorinsky constant (see, e.g., Germano et al. [15], Moin et al. [31] and Piomelli [32]).

In our approach we invoke scale separation *ab initio*. We apply the variational multiscale approach to a space-time formulation of the incompressible Navier–Stokes equations. From the discrete point of view, this leads to the (time-) discontinuous Galerkin method on space-time slabs. This procedure proves convenient for our purposes and obviates the need to consider specific time discretization (i.e., ODE) algorithms. We note, however, that it is a straightforward matter to develop traditional semi-discrete approaches with similar

* The Mary and Gordon Crary Family Professor of Engineering and Chairman of the Division of Mechanics and Computation
** Graduate Research Assistant
*** Assistant Professor of Mechanical and Aerospace Engineering

properties to the ones descried here. See Appendix A for a sketch.

By virtue of the fact that we explicitly derive equations governing large *and* small scales, certain terms appear which are not present in the classical filtered Navier–Stokes equations. In particular, we may mention what may be described as the small-scale Reynolds stress. This may be thought of as the difference between the unfiltered and filtered tensor product of velocity fluctuations, viz.,

$$\left(\boldsymbol{u}'\otimes\boldsymbol{u}'\right)' = \boldsymbol{u}'\otimes\boldsymbol{u}' - \overline{(\boldsymbol{u}'\otimes\boldsymbol{u}')}.$$

(Note that the filtered quantity is the classical Reynolds stress.) We ascribe the rapidly fluctuating nature of turbulence to the small-scale Reynolds stress and conclude that its effect must be modeled, unless we are prepared to resolve all scales by way of Direct Numerical Simulation (DNS).

In our approach, modeling may be performed without omitting the term whose effect we are modeling because there is no closure problem in the variational formulation. This may be contrasted with the traditional LES approach in which the entire subgrid-scale stress needs to be modeled due to the closure problem engendered by filtering. We account for all other effects exactly, in particular, Leonard stress, classical Reynolds stress and cross-stress terms. Recent results suggest that this may be advantageous (see Salvetti and Banarjee [34], Salvetti et al. [36], and Salvetti and Beux [35]).

The small-scale Reynolds stress has a remarkable property: despite being the generator of rapid fluctuations, which are eventually consumed by molecular viscous dissipation, its *direct* effect on kinetic energy decay is zero. Consequently, it may be omitted from the equations without upsetting the global *a priori* kinetic energy decay inequality which we pay careful attention to throughout. However, its *indirect* effect on kinetic energy decay is then lost, suggesting it should be modeled by a dissipative mechanism. To this end we consider two simple generalizations of the Smagorinsky eddy viscosity model which act only on small scales. One is completely desensitized to large-scale behavior, the other, partially desensitized. Parameters are again estimated by way of the approach due to Lilly [28–30].

We speculate that, because scale separation has been invoked from the outset, a constant-coefficient model in the present approach may have validity for a greater variety of flows than does the classical LES/constant-coefficient Smagorinsky model. As this is our *only* modeling assumption and it involves somewhat *ad hoc* generalizations of the classical Smagorinsky model, possible improvement in our approach may focus on this single issue. In summarizing our approach we contrast it with the work of the Temam group (see, e.g., Dubois et al. [9, 10]).

We also include a section of remarks for the finite element cognoscenti about implementational issues.

Finally, we draw conclusions. In particular, we review how the present approach addresses criticisms of the classical LES/Smagorinsky method and identify some other useful properties.

2 Incompressible Navier–Stokes equations

Let Ω be an open, connected, bounded subset of $\mathbb{R}^d$, $d = 2$ or 3, with piecewise smooth boundary $\Gamma = \partial\Omega$; Ω represents the fixed spatial domain of our problem. The time interval of interest is denoted $]0, T[$, $T > 0$, and thus the space-time domain is $\mathsf{Q} = \Omega \times]0, T[$; its lateral boundary is denoted $\mathsf{P} = \Gamma \times]0, T[$. The setup is illustrated in Fig. 1.

The initial/boundary-value problem consists of solving the following equations for $\boldsymbol{u} : \overline{\mathsf{Q}} \to \mathbb{R}^d$, the velocity, and $p : \mathsf{Q} \to \mathbb{R}$, the pressure (divided by density),

$$\frac{\partial \boldsymbol{u}}{\partial t} + \nabla\cdot(\boldsymbol{u}\otimes\boldsymbol{u}) + \nabla p = \nu\Delta\boldsymbol{u} + \boldsymbol{f} \quad \text{in } \mathsf{Q} \tag{1}$$

$$\nabla\cdot\boldsymbol{u} = 0 \quad \text{in } \mathsf{Q} \tag{2}$$

$$\boldsymbol{u} = \boldsymbol{0} \quad \text{on } \mathsf{P} \tag{3}$$

$$\boldsymbol{u}(0^+) = \boldsymbol{u}(0^-) \quad \text{on } \Omega \tag{4}$$

where $\boldsymbol{f} : \mathsf{Q} \to \mathbb{R}^d$ is the given body force (per unit volume); ν is the kinematic viscosity, assumed positive and constant; $\boldsymbol{u}(0^-) : \Omega \to \mathbb{R}^d$ is the given initial velocity; and $\otimes$ denotes the tensor product (e.g., in component notation $[\boldsymbol{u}\otimes\boldsymbol{v}]_{ij} = u_i v_j$). Equations (1)–(4) are, respectively, the linear momentum balance, the incompressibility constraint, the no-slip boundary condition and the initial condition.

Note that when we write a function with only one argument, it is assumed to refer to time. For example, $\boldsymbol{u}(t) = \boldsymbol{u}(\cdot, t)$, where the spatial argument $\boldsymbol{x} \in \Omega$ is suppressed for simplicity. Furthermore,

$$\boldsymbol{u}\left(t^{\pm}\right) = \lim_{\varepsilon\downarrow 0} \boldsymbol{u}\left(t \pm \varepsilon\right) \quad \forall t \in [0, T]\,. \tag{5}$$

This notation allows us to distinguish between $\boldsymbol{u}(0^+)$ and $\boldsymbol{u}(0^-)$, the solution and its given initial value, respectively. In our variational formulation of the initial/boundary-value problem (see Sect. 6) we will only satisfy (4) in a weak sense. The notation of (4) and (5) is also conducive to the generalization of the formulation to the discrete case in which we pose the numerical problem in terms of a sequence of "space-time slabs", where the solution may be discontinuous across the slab interfaces.

For mathematical results of existence, uniqueness and regularity, we refer to Temam [39]. See also Quarteroni and Valli [33], and references therein.

We are interested in solutions of (1)–(4) for the case in which ν is very small, which typically gives rise to turbulence, an inherently chaotic and unpredictable phenomenon.

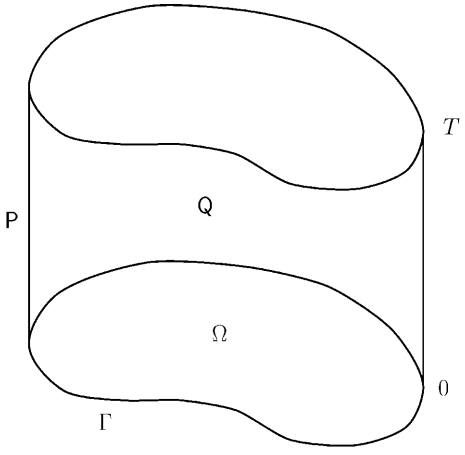

Fig. 1. Space-time domain for the initial/boundary-value problem

Nevertheless, some statistical quantities, such as particular spatial and temporal averages, are deterministic and, in principle, computable.

3 Large Eddy Simulation (LES)

The unpredictability of turbulence suggests reformulating the initial/boundary-value problem in terms of averaged quantities. In Large Eddy Simulation (LES) a spatial averaging procedure is employed. For example, let

$$\overline{\boldsymbol{u}}(\boldsymbol{x},t)=\int_{D_\Delta(\boldsymbol{x})} g(\boldsymbol{x},\boldsymbol{y})\boldsymbol{u}(\boldsymbol{y},t)\,d\boldsymbol{y} \tag{6}$$

in which

$$g(\boldsymbol{x},\boldsymbol{y})=g(\boldsymbol{x}-\boldsymbol{y}) \qquad \text{(homogeneity)} \tag{7}$$

and

$$1=\int_{D_\Delta(\boldsymbol{x})} g(\boldsymbol{x},\boldsymbol{y})\,d\boldsymbol{y} \tag{8}$$

where $\overline{\boldsymbol{u}}$ is the filtered velocity and g is the filter having support in $D_\Delta(\boldsymbol{x})\subset\Omega$, a neighborhood of $\boldsymbol{x}\in\Omega$. (See Fig. 2 for a schematic of a candidate filter.)

The size of $D_\Delta(\boldsymbol{x})$ is characterized by Δ, the filter width. There are various possibilities for $D_\Delta(\boldsymbol{x})$. For example, we may take

$$D_\Delta(\boldsymbol{x})=\left\{\boldsymbol{y}\in\mathbb{R}^d \mid \rho(\boldsymbol{x},\boldsymbol{y})<\Delta/2\right\}. \tag{9}$$

The distance function, ρ, may be defined in terms of the Euclidean norm, in which case $D_\Delta(\boldsymbol{x})$ is an open ball of radius $\Delta/2$ centered at $\boldsymbol{x}$.

The effect of filtering is schematically illustrated in Fig. 3.

The filtered field, $\overline{\boldsymbol{u}}$, is commonly referred to as the large, coarse, or resolvable scales. It is assumed adequate to represent the larger structures of the flow. The difference between $\boldsymbol{u}$ and $\overline{\boldsymbol{u}}$, i.e.,

$$\boldsymbol{u}'=\boldsymbol{u}-\overline{\boldsymbol{u}} \tag{10}$$

is the rapidly fluctuating part of $\boldsymbol{u}$; $\boldsymbol{u}'$ is commonly referred to as the small, fine, or unresolvable scales. Although we are primarily interested in computing $\overline{\boldsymbol{u}}$, due to the nonlinear nature of the Navier–Stokes equations, the effect of $\boldsymbol{u}'$ on $\overline{\boldsymbol{u}}$ cannot be ignored.

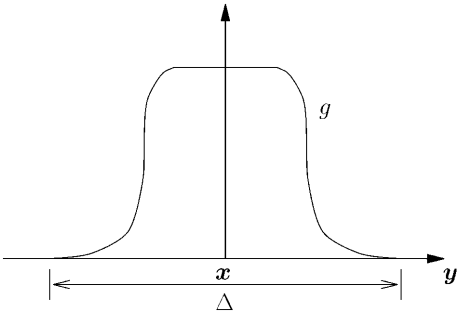

Fig. 2. Typical filter function for LES

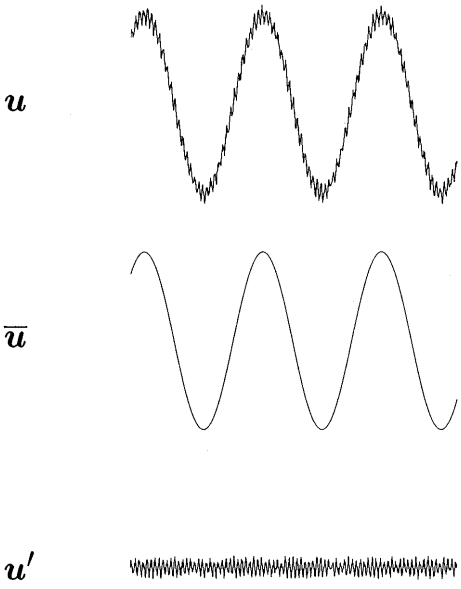

Fig. 3. The effect of filtering

Remark. The homogeneous structure of the filter results in the commutativity of spatial differentiation and filtering, a property exploited in the derivation of the equations governing filtered quantities. However, in order to obtain the filtered equations corresponding to (1)–(4), we need to perform the filtering operation about all $\boldsymbol{x}\in\Omega$, and in particular for $\boldsymbol{x}\in\Omega\backslash\Omega_\Delta$, where

$$\Omega_\Delta=\{\boldsymbol{x} \mid D_\Delta(\boldsymbol{x})\subset\Omega\}. \tag{11}$$

In this case, the support of the filtering operation extends beyond the boundary of Ω. For an illustration, see Fig. 4. Clearly, this creates mathematical ambiguities. (Note that this problem does not arise in cases of domains with periodic boundary conditions.) An alternative approach is to reduce the size of the filter as the boundary is approached, but this too creates mathematical complications. It is not our intent to address this issue further herein. We wish to emphasize, though, that it is an issue. (For recent literature concerning this problem, see Galdi and Layton [14], John and Layton [26], Layton [27], and Ghosal and Moin [16].)

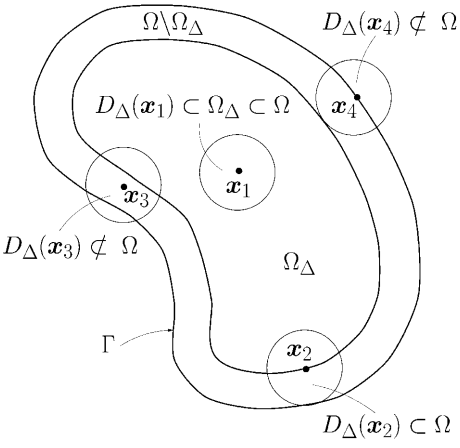

Fig. 4. The support of the filter extends beyond the boundary of Ω

3.1 Filtered Navier–Stokes equations

The filtered equations corresponding to (1)–(4) are assumed to take the form

$$\frac{\partial \overline{\boldsymbol{u}}}{\partial t} + \nabla \cdot (\overline{\boldsymbol{u} \otimes \boldsymbol{u}}) + \nabla \overline{p} = \nu \Delta \overline{\boldsymbol{u}} + \overline{\boldsymbol{f}} \quad \text{in } \mathsf{Q} \tag{12}$$

$$\nabla \cdot \overline{\boldsymbol{u}} = 0 \quad \text{in } \mathsf{Q} \tag{13}$$

$$\overline{\boldsymbol{u}} = \boldsymbol{0} \quad \text{on } \mathsf{P} \tag{14}$$

$$\overline{\boldsymbol{u}}(0^+) = \overline{\boldsymbol{u}}(0^-) \quad \text{on } \Omega. \tag{15}$$

The nonlinear term in (12) gives rise to a *closure problem*: how to compute $\overline{\boldsymbol{u} \otimes \boldsymbol{u}}$? This necessarily entails some form of approximation. To this end, define the *subgrid-scale stress*

$$\boldsymbol{T} = \overline{\boldsymbol{u}} \otimes \overline{\boldsymbol{u}} - \overline{\boldsymbol{u} \otimes \boldsymbol{u}}. \tag{16}$$

In terms of the subgrid-scale stress, the filtered momentum equation (12) is rewritten as

$$\frac{\partial \overline{\boldsymbol{u}}}{\partial t} + \nabla \cdot (\overline{\boldsymbol{u}} \otimes \overline{\boldsymbol{u}}) + \nabla \overline{p} = \nu \Delta \overline{\boldsymbol{u}} + \nabla \cdot \boldsymbol{T} + \overline{\boldsymbol{f}}. \tag{17}$$

Thus, $\boldsymbol{T}$ needs to be modeled to close the system. To be more precise, only the deviatoric part of $\boldsymbol{T}$, namely,

$$\operatorname{dev} \boldsymbol{T} = \boldsymbol{T} - \left(\tfrac{1}{3} \operatorname{tr} \boldsymbol{T}\right) \boldsymbol{I}, \tag{18}$$

where $\boldsymbol{I}$ is the identity tensor, needs to be modeled, and the dilatational part, $\frac{1}{3} \operatorname{tr} \boldsymbol{T}$, may be subsumed by $\overline{p}$.

4 Smagorinsky closure

The classical and most widely used closures are based on the *Smagorinsky eddy viscosity model* [37]:

$$\boldsymbol{T}_S = 2 \nu_T \nabla^s \overline{\boldsymbol{u}} \tag{19}$$

where

$$\nu_T = (C_S \Delta)^2 \left| \nabla^s \overline{\boldsymbol{u}} \right| \tag{20}$$

$$\nabla^s \overline{\boldsymbol{u}} = \tfrac{1}{2} \left(\nabla \overline{\boldsymbol{u}} + (\nabla \overline{\boldsymbol{u}})^T \right) \tag{21}$$

$$\left| \nabla^s \overline{\boldsymbol{u}} \right| = \left(2 \nabla^s \overline{\boldsymbol{u}} \cdot \nabla^s \overline{\boldsymbol{u}} \right)^{1/2} \tag{22}$$

and C_S is referred to as the *Smagorinsky constant*. Note, $\boldsymbol{T}_S$ is deviatoric, i.e., $\boldsymbol{T}_S = \operatorname{dev} \boldsymbol{T}_S$.

Various criticisms have been lodged against the Smagorinsky model (see, e.g., Germano et al. [15], and Piomelli [32]). Typical of these are:

1. $\boldsymbol{T}_S$ does not replicate the asymptotic behavior of $\boldsymbol{T}$ near walls, in particular, $\boldsymbol{T}_S$ does not vanish at walls.

2. Values of C_S obtained from the decay of homogeneous isotropic turbulence tend to be *too large* for other situations, such as in the presence of mean shear.

3. $\boldsymbol{T}_S$ precludes *backscatter* (energy flow from small to large scales) which can be significant in some cases.

4. $\boldsymbol{T}_S$ produces *excessive damping* of resolved structures in transition, resulting in incorrect growth rate of perturbations.

As a result of these shortcomings, many modifications have been proposed, such as wall functions, intermittency functions, etc. Perhaps the most notable advancement is the *dynamic subgrid-scale model* (Germano et al. [15]), in which it is assumed that C_S is a function, i.e.,

$$C_S = C_S(\boldsymbol{x}, t). \tag{23}$$

The identification of C_S is performed adaptively by sampling the smallest resolved scales and using this information to model the subgrid scales. The dynamic model has been applied to a variety of flows and improved results have been obtained in most cases. For a recent review of the state-of-the-art and assessment, see Piomelli [32]. It is a widely held opinion that any proposal of a new LES model based on the Smagorinsky concept must address, at the very least, the shortcomings delineated above.

4.1 Estimation of parameters

The Smagorinsky parameters C_S and Δ may be determined by a procedure due to Lilly [28–30]. In Lilly's analysis it is assumed that turbulent kinetic energy production and dissipation are in balance. The limit of resolution is assumed to fall in the Kolmogorov inertial subrange and $|\nabla^s \overline{\boldsymbol{u}}|$ is determined by spectral integration. This enables quantification of $C_S \Delta$ and ν_T. A brief summary of the steps involved follows.

Consider Fig. 5. $E(k)$ is the spectral amplitude of kinetic energy, defined as the integral over surfaces of spheres in wave-number space parametrized by the radius k. In the inertial subrange

$$E(k) = \alpha \varepsilon^{2/3} k^{-5/3} \tag{24}$$

where α is the Kolmogorov constant and ε is the turbulent dissipation. $|\nabla^s \overline{\boldsymbol{u}}|$ may be determined from the relation

$$\tfrac{1}{2} \left| \nabla^s \overline{\boldsymbol{u}} \right|^2 = \int_0^{\bar{k}} k^2 E(k) \, dk \tag{25}$$

where $\bar{k}$ corresponds to the resolution limit, which is the cut-off wave number for spectral discretization. Equating turbulent kinetic energy dissipation with dissipation produced

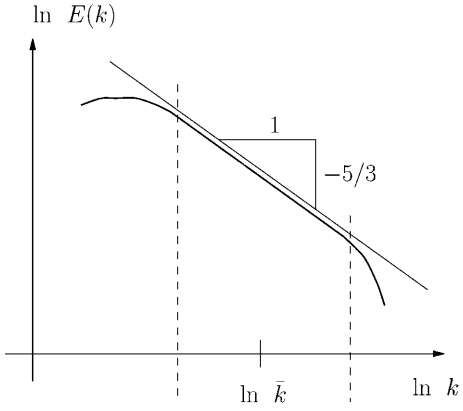

Fig. 5. Kolmogorov energy spectrum

by the Smagorinsky model, and evaluating (25) using (24), yields

$$\varepsilon = \boldsymbol{T}_S \cdot \nabla^s \overline{\boldsymbol{u}} = 2(C_S\Delta)^2 \left|\nabla^s \overline{\boldsymbol{u}}\right| \left(\nabla^s \overline{\boldsymbol{u}} \cdot \nabla^s \overline{\boldsymbol{u}}\right)$$
$$= (C_S\Delta)^2 \left|\nabla^s \overline{\boldsymbol{u}}\right|^3 = (C_S\Delta)^2 \left(\frac{3\alpha}{2}\right)^{3/2} \bar{k}^2 \varepsilon \tag{26}$$

from which it follows that

$$C_S\Delta = \left(\frac{2}{3\alpha}\right)^{3/4} \bar{k}^{-1} \tag{27}$$

and

$$\nu_T = \left(\frac{2}{3\alpha}\right) \varepsilon^{1/3}\, \bar{k}^{-4/3}. \tag{28}$$

Assuming $\bar{k} = \text{const}\, \bar{h}^{-1}$, where $\bar{h}$ is the mesh parameter, it follows from (27) and (28) that

$$C_S\Delta = O(\bar{h}) \tag{29}$$

and

$$\nu_T = O(\bar{h}^{4/3}). \tag{30}$$

Remarks.

1. Assuming $\Delta = \bar{h} = \pi\bar{k}^{-1}$ and $\alpha = 1.4$, it follows from (27) that $C_S \cong 0.18$, a value which proves satisfactory for homogeneous isotropic turbulence. However, it has been noted that smaller values, often around 0.10, have been required for other applications (see Germano et al. [15]).

2. The excessive damping of resolved structures may be explained by (19) and (30). An $O(\bar{h}^{4/3})$ viscosity acts on all scales present. It is known from the analysis of artificial viscosity methods that, even for linear model problems, an $O(\bar{h}^{4/3})$ artificial viscosity results in convergence that is at most $O(\bar{h}^{4/3})$ in L_2 and $O(\bar{h}^{2/3})$ in H^1. This is indeed very slow convergence and is deemed by most analysts as unacceptable. Furthermore, these results are probably optimistic for the (nonlinear) Navier–Stokes equations. The physical design of the Smagorinsky model results in the correct extraction of total kinetic energy, but the flaw seems to be that the extraction of kinetic energy occurs in all scales and, in particular, in the so-called "resolved scales".

3. The analysis described assumed an isotropic discretization. The anisotropic case has also been addressed by Lilly [30].

5 Review of some computational experiments

The Smagorinsky model is capable of representing both the $k^{-5/3}$ law and the theoretical decay of kinetic energy with time for homogeneous isotropic turbulence. This is observed for some centered finite difference schemes, Galerkin finite element methods, and spectral methods. In the context of finite element methods, the studies of Chalot et al. [7] are very illuminating. They employed an industrial-strength CFD code based on a stabilized finite element procedure of GLS/SUPG type. By shutting off the stabilization terms, a standard Galerkin method is obtained. They performed calculations of turbulent flows with and without stabilization, and with and without the Smagorinsky term, in all combinations. Some of their observations are summarized as follows:

1. The Galerkin finite element method with the Smagorinsky model produced the correct $k^{-5/3}$ energy spectrum and the $t^{-1.4}$ decay of kinetic energy for homogeneous isotropic turbulence (see Fig. 6). The value of the Smagorinsky constant used was 0.18246.

2. The same calculation with the addition of the stabilization also resulted in the $t^{-1.4}$ decay of kinetic energy, but deviated from the $k^{-5/3}$ energy spectrum at high wave numbers. See Fig. 7. This was attributed to the residual-based algorithmic dissipation produced by the stabilization term, which is known to attenuate high wave-number modes while retaining good accuracy for low wave numbers. (This is to be contrasted with classical artificial-diffusion and upwind methods which also strongly attenuate low wave-number modes.)

3. The stabilized method without the Smagorinsky term did not replicate the $k^{-5/3}$ law. Consequently, it is concluded that this form of algorithmic dissipation does not act as a true physical subgrid-scale model.

4. The calculation of a mixing layer with the same Smagorinsky model proved to be too dissipative, as anticipated. This was attributed to the fact that the Smagorinsky model is incapable of discriminating between the mean shear and the shear associated with fluctuations. A modification, due

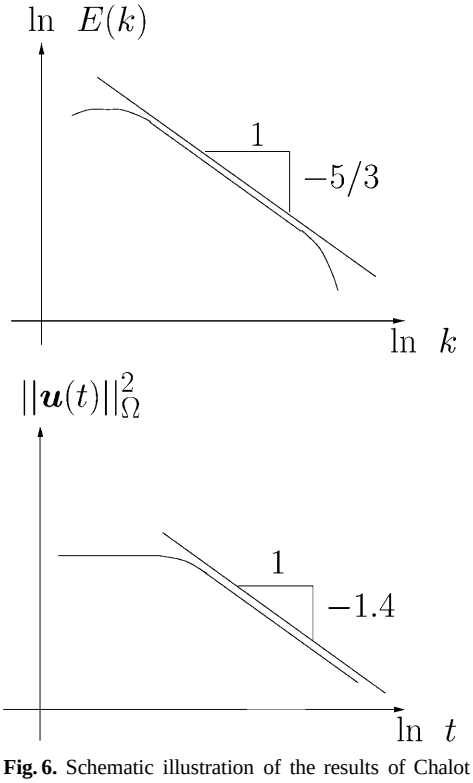

Fig. 6. Schematic illustration of the results of Chalot et al. [7] for homogeneous isotropic turbulence using a Galerkin finite element method with Smagorinsky model

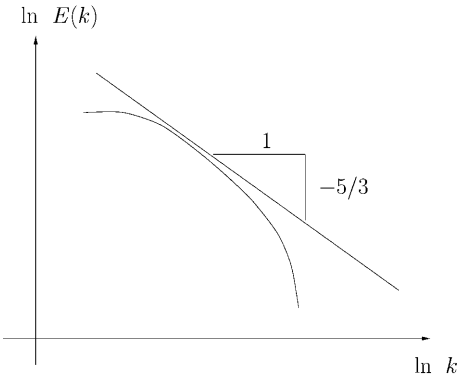

Fig. 7. Schematic illustration of the results of Chalot et al. [7] for homogeneous isotropic turbulence using a finite element method with algorithmic dissipation in conjunction with the Smagorinsky model (cf. Fig. 6)

to David [8], which measured this effect and reduced the Smagorinsky constant accordingly, produced significant improvements. This example is sometimes used as motivation for dynamic modeling of the constant. We wish to propose an alternative interpretation: It may not be the constant which needs to be changed but rather the dependence of the Smagorinsky model on the resolved scales $\overline{\boldsymbol{u}}$. We shall explore this line of thinking subsequently in the context of the variational multiscale method.

These observations are consistent with the criticisms of the Smagorinsky model delineated previously and provide additional insights into the requirements which need to be satisfied by finite element methods in LES applications.

The studies of Chalot et al. [7] complement earlier observations of Jansen [24], who also employed a stabilized method of GLS/SUPG type. The results of Jansen are consistent with those of Chalot et al. when the stabilized method is combined with the Smagorinsky model. Jansen also observed that the stabilized method without the Smagorinsky model did not represent a physical subgrid-scale model in that the dissipation was underestimated due to significant accumulation of energy in high wave numbers. However, the stabilized method combined with dynamic modeling performed better than the static model, achieving correct equilibrium dissipation.

6 Variational multiscale method

6.1 Space-time formulation of the incompressible Navier–Stokes equations

We consider a Galerkin space-time formulation with weakly imposed initial condition. Let $\mathcal{V} = \mathcal{V}(\mathsf{Q})$ denote the trial solution and weighting function spaces, which are assumed to be identical. We assume $\boldsymbol{U} = \{\boldsymbol{u}, p\} \in \mathcal{V}$ implies $\boldsymbol{u} = \boldsymbol{0}$ on P and $\int_\Omega p(t)\, d\Omega = 0$ for all $t \in]0, T[$. The variational formulation is stated as follows:
Find $\boldsymbol{U} \in \mathcal{V}$ such that $\forall \boldsymbol{W} = \{\boldsymbol{w}, q\} \in \mathcal{V}$

$$B(\boldsymbol{W}, \boldsymbol{U}) = (\boldsymbol{W}, \boldsymbol{F}) \tag{31}$$

where

$$\begin{aligned} B(\boldsymbol{W}, \boldsymbol{U}) = {} & \left(\boldsymbol{w}(T^-), \boldsymbol{u}(T^-)\right)_\Omega - \left(\frac{\partial \boldsymbol{w}}{\partial t}, \boldsymbol{u}\right)_{\mathsf{Q}} \\ & - (\nabla \boldsymbol{w}, \boldsymbol{u} \otimes \boldsymbol{u})_{\mathsf{Q}} + (q, \nabla \cdot \boldsymbol{u})_{\mathsf{Q}} \\ & - (\nabla \cdot \boldsymbol{w}, p)_{\mathsf{Q}} + \left(\nabla^s \boldsymbol{w}, 2\nu \nabla^s \boldsymbol{u}\right)_{\mathsf{Q}} \end{aligned} \tag{32}$$

and

$$(\boldsymbol{W}, \boldsymbol{F}) = (\boldsymbol{w}, \boldsymbol{f})_{\mathsf{Q}} + \left(\boldsymbol{w}(0^+), \boldsymbol{u}(0^-)\right)_\Omega \tag{33}$$

This formulation implies weak satisfaction of the momentum equations and incompressibility constraint, in addition to the initial condition. The boundary condition is built into the definition of $\mathcal{V}$.

Remarks.

1. $\boldsymbol{u}(0^-)$ is viewed as known when computing the solution in Q.
2. The standard discontinuous Galerkin method with respect to time is obtained by replacing $[0, T]$ by $[t_n, t_{n+1}]$, $n = 0, 1, 2, \ldots$ and summing over the space-time slabs

$$\mathsf{Q}_n = \Omega \times]t_n, t_{n+1}[. \tag{34}$$

In this case we view (31)–(33) as the variational equation for a typical slab.
3. The conditions $\nabla \cdot \boldsymbol{u} = 0$ on Q and $\boldsymbol{u} = \boldsymbol{0}$ on P imply

$$(\nabla \boldsymbol{u}, \boldsymbol{u} \otimes \boldsymbol{u})_{\mathsf{Q}} = 0. \tag{35}$$

In the discrete case this term may need to be altered to preserve this property. See Quarteroni and Valli [33], p.435.

Kinetic energy decay inequality. Substitution of $\boldsymbol{U}$ for $\boldsymbol{W}$ in (31) leads to the inequality

$$\tfrac{1}{2} \left|\left|\boldsymbol{u}(T^-)\right|\right|_\Omega^2 + 2\nu \left|\left|\nabla^s \boldsymbol{u}\right|\right|_{\mathsf{Q}}^2 \le \tfrac{1}{2} \left|\left|\boldsymbol{u}(0^-)\right|\right|_\Omega^2 + (\boldsymbol{u}, \boldsymbol{f})_{\mathsf{Q}} \tag{36}$$

from which follows

$$\tfrac{1}{2} \left|\left|\boldsymbol{u}(T^-)\right|\right|_\Omega^2 + \nu \left|\left|\nabla^s \boldsymbol{u}\right|\right|_{\mathsf{Q}}^2 \le \tfrac{1}{2} \left|\left|\boldsymbol{u}(0^-)\right|\right|_\Omega^2 + \frac{C_\Omega}{4\nu} \left|\left|\boldsymbol{f}\right|\right|_{\mathsf{Q}}^2, \tag{37}$$

where C_Ω is the constant in the Poincaré inequality:

$$||\boldsymbol{u}||_\Omega^2 \le C_\Omega \left|\left|\nabla^s \boldsymbol{u}\right|\right|_\Omega^2. \tag{38}$$

6.2 Separation of scales

Let

$$\mathcal{V} = \overline{\mathcal{V}} \oplus \mathcal{V}' \tag{39}$$

where $\overline{\mathcal{V}}$ is identified with a standard *finite element space*. Various characterizations of $\mathcal{V}'$ are possible. Note that $\mathcal{V}'$ is

∞-dimensional. In the discrete case, $\mathcal{V}'$ can be replaced with various finite-dimensional approximations, such as hierarchical polynomial refinement, bubbles, etc. In any case, (39) enables us to decompose (31) into two sub-problems:

$$B\left(\overline{\boldsymbol{W}}, \overline{\boldsymbol{U}}+\boldsymbol{U}'\right) = \left(\overline{\boldsymbol{W}}, \boldsymbol{F}\right) \tag{40}$$

$$B\left(\boldsymbol{W}', \overline{\boldsymbol{U}}+\boldsymbol{U}'\right) = \left(\boldsymbol{W}', \boldsymbol{F}\right) \tag{41}$$

where

$$\boldsymbol{U} = \overline{\boldsymbol{U}} + \boldsymbol{U}' \tag{42}$$

$$\boldsymbol{W} = \overline{\boldsymbol{W}} + \boldsymbol{W}' \tag{43}$$

in which $\overline{\boldsymbol{U}}, \overline{\boldsymbol{W}} \in \overline{\mathcal{V}}$ and $\boldsymbol{U}', \boldsymbol{W}' \in \mathcal{V}'$.

Remark. It is important to realize that although we continue to use the over-bar and prime notations to connote large and small scales, the meaning is somewhat different than for the classical LES formulation considered previously. Here $\overline{\boldsymbol{U}}$ and $\boldsymbol{U}'$ may be thought of as "projections" of $\boldsymbol{U}$ onto $\overline{\mathcal{V}}$ and $\mathcal{V}'$, respectively. We use the terminology "projections" loosely because $\overline{\boldsymbol{U}}$ and $\boldsymbol{U}'$ are obtained from $\boldsymbol{U}$ by solving coupled nonlinear problems, viz.,

$$B\left(\overline{\boldsymbol{W}}, \overline{\boldsymbol{U}}+\boldsymbol{U}'\right) = B\left(\overline{\boldsymbol{W}}, \boldsymbol{U}\right) \tag{44}$$

$$B\left(\boldsymbol{W}', \overline{\boldsymbol{U}}+\boldsymbol{U}'\right) = B\left(\boldsymbol{W}', \boldsymbol{U}\right). \tag{45}$$

Consequently, it is not possible to identify a simple filtering relationship between $\overline{\boldsymbol{U}}$ and $\boldsymbol{U}$, such as (6)–(7). Nevertheless, $\overline{\boldsymbol{U}}$ represents the part of $\boldsymbol{U}$ which lives in $\overline{\mathcal{V}}$, and thus clearly is a large-scale representation of $\boldsymbol{U}$. Likewise, $\boldsymbol{U}'$ is a small-scale representation of $\boldsymbol{U}$. The relationship between the present $\overline{\boldsymbol{U}}$ and its filtered counterpart is in our opinion a complex mathematical problem. We again refer to Galdi and Layton [14] and John and Layton [26] for initiatory attempts at its resolution.

Let

$$B_1\left(\boldsymbol{W}, \overline{\boldsymbol{U}}, \boldsymbol{U}'\right) = \frac{d}{d\varepsilon} B\left(\boldsymbol{W}, \overline{\boldsymbol{U}}+\varepsilon\boldsymbol{U}'\right)\Big|_{\varepsilon=0} \tag{46}$$

$$B_2\left(\boldsymbol{W}, \overline{\boldsymbol{U}}, \boldsymbol{U}'\right) = \frac{d^2}{d\varepsilon^2} B\left(\boldsymbol{W}, \overline{\boldsymbol{U}}+\varepsilon\boldsymbol{U}'\right)\Big|_{\varepsilon=0}. \tag{47}$$

With these we may write

$$B\left(\boldsymbol{W}, \overline{\boldsymbol{U}}+\boldsymbol{U}'\right) = B(\boldsymbol{W}, \overline{\boldsymbol{U}}) + B_1(\boldsymbol{W}, \overline{\boldsymbol{U}}, \boldsymbol{U}') + \tfrac{1}{2} B_2(\boldsymbol{W}, \overline{\boldsymbol{U}}, \boldsymbol{U}') \tag{48}$$

where

$$\tfrac{1}{2} B_2(\boldsymbol{W}, \overline{\boldsymbol{U}}, \boldsymbol{U}') = -\left(\nabla \boldsymbol{w}, \boldsymbol{u}' \otimes \boldsymbol{u}'\right)_{\mathsf{Q}} \tag{49}$$

and

$$\begin{aligned} B_1(\boldsymbol{W}, \overline{\boldsymbol{U}}, \boldsymbol{U}') = {} & \left(\boldsymbol{w}(T^-), \boldsymbol{u}'(T^-)\right)_{\Omega} - \left(\frac{\partial \boldsymbol{w}}{\partial t}, \boldsymbol{u}'\right)_{\mathsf{Q}} \\ & - \left(\nabla \boldsymbol{w}, \overline{\boldsymbol{u}} \otimes \boldsymbol{u}' + \boldsymbol{u}' \otimes \overline{\boldsymbol{u}}\right)_{\mathsf{Q}} \\ & + \left(q, \nabla \cdot \boldsymbol{u}'\right)_{\mathsf{Q}} - \left(\nabla \cdot \boldsymbol{w}, p'\right)_{\mathsf{Q}} \\ & + \left(\nabla^s \boldsymbol{w}, 2\nu \nabla^s \boldsymbol{u}'\right)_{\mathsf{Q}}. \end{aligned} \tag{50}$$

Remark. $B_1(\boldsymbol{W}, \overline{\boldsymbol{U}}, \boldsymbol{U}')$ is the *linearized* Navier–Stokes operator.

With the aid of (48)–(50) we may rewrite (40) and (41) as

$$B(\overline{\boldsymbol{W}}, \overline{\boldsymbol{U}}) + B_1(\overline{\boldsymbol{W}}, \overline{\boldsymbol{U}}, \boldsymbol{U}') = (\nabla \overline{\boldsymbol{w}}, \boldsymbol{u}' \otimes \boldsymbol{u}')_{\mathsf{Q}} + \left(\overline{\boldsymbol{W}}, \boldsymbol{F}\right) \tag{51}$$

$$B_1(\boldsymbol{W}', \overline{\boldsymbol{U}}, \boldsymbol{U}') - (\nabla \boldsymbol{w}', \boldsymbol{u}' \otimes \boldsymbol{u}')_{\mathsf{Q}} = -\left[B(\boldsymbol{W}', \overline{\boldsymbol{U}}) - \left(\boldsymbol{W}', \boldsymbol{F}\right)\right]. \tag{52}$$

This amounts to a pair of coupled, nonlinear variational equations. Given the small scales (i.e., $\boldsymbol{U}'$), (51) enables solution for the large scales (i.e., $\overline{\boldsymbol{U}}$). Likewise, the large scales drive the small scales through (52). Note, the right hand side of (52) is the *residual of the large scales projected onto* $\mathcal{V}'$.

Remark. The subgrid-scale stress, $\boldsymbol{T}$ (see (16)), may be decomposed into the Reynolds stress, cross stress and Leonard stress. In the variational formulation, the analogs of these terms are:

$$\left(\nabla \overline{\boldsymbol{w}}, \boldsymbol{u}' \otimes \boldsymbol{u}'\right)_{\mathsf{Q}} \qquad \text{(Reynolds stress)} \tag{53}$$

$$\left(\nabla \overline{\boldsymbol{w}}, \overline{\boldsymbol{u}} \otimes \boldsymbol{u}' + \boldsymbol{u}' \otimes \overline{\boldsymbol{u}}\right)_{\mathsf{Q}} \qquad \text{(Cross stress)} \tag{54}$$

$$(\nabla \overline{\boldsymbol{w}}, \overline{\boldsymbol{u}} \otimes \overline{\boldsymbol{u}})_{\mathsf{Q}} - (\nabla \boldsymbol{w}, \overline{\boldsymbol{u}} \otimes \overline{\boldsymbol{u}})_{\mathsf{Q}} = -\left(\nabla \boldsymbol{w}', \overline{\boldsymbol{u}} \otimes \overline{\boldsymbol{u}}\right)_{\mathsf{Q}} \qquad \text{(Leonard stress)} \tag{55}$$

Note that (53)–(54) appear in (51), and (55) appears in the right-hand side of (52). We wish to point out that up to this point our results are *exact*, i.e., nothing has been omitted and no modeling has been performed.

6.3 Modeling of subgrid scales

In the continuous case, the term $\left(\nabla \boldsymbol{w}', \boldsymbol{u}' \otimes \boldsymbol{u}'\right)_{\mathsf{Q}}$ is responsible for the *rapidly fluctuating* behavior of the small scales. Its effect cannot be accurately represented in the discrete case without resorting to excessive resolution, amounting to Direct Numerical Simulation (DNS). It is interesting to note that although $\left(\nabla \boldsymbol{w}', \boldsymbol{u}' \otimes \boldsymbol{u}'\right)_{\mathsf{Q}}$ is *indirectly* responsible for turbulent kinetic energy decay through the creation of small scales which are dissipated through molecular viscosity, it has *no* direct effect on the kinetic energy decay inequality because

$$\left(\nabla \boldsymbol{u}', \boldsymbol{u}' \otimes \boldsymbol{u}'\right)_{\mathsf{Q}} = 0 \tag{56}$$

owing to $\nabla \cdot \boldsymbol{u}' = 0$ in Q and $\boldsymbol{u}' = \boldsymbol{0}$ on P. We reiterate the point made immediately after (35) that, in the discrete case, the form of this term may need to be altered to ensure this property (Quarteroni and Valli [33], p.435). Consequently, it is our intent to model $\left(\nabla \boldsymbol{w}', \boldsymbol{u}' \otimes \boldsymbol{u}'\right)_{\mathsf{Q}}$ in the discrete case. Specifically, we shall account for its effect by adding an eddy viscosity model, inspired by the form of the Smagorinsky model.

Remark. Observe that closure is not the motivation for modeling in the case of the variational multiscale formulation. In fact, there is *no* closure problem whatsoever. The need for modeling is due simply to the inability of typical discrete approximations to properly represent all necessary scales. We view this as a significant advantage of projection/variational methods over the classical filtered equation approach because it eliminates the necessity of modeling the entire subgrid-scale stress $\boldsymbol{T}$ and reduces the modeling problem to accounting for the viscous dissipation of missing small scales.

Thus, we add $\left(\nabla \boldsymbol{w}', \boldsymbol{R}'_S\right)_{\mathrm{Q}}$ to (52), where

$$\boldsymbol{R}'_S = 2\nu'_T \nabla^s \boldsymbol{u}'. \tag{57}$$

[We shall postpone, for the moment, specification of ν'_T.] The end result is

$$B'(\boldsymbol{W}', \overline{\boldsymbol{U}}, \boldsymbol{U}') = -\left[B(\boldsymbol{W}', \overline{\boldsymbol{U}}) - \left(\boldsymbol{W}', \boldsymbol{F}\right)\right] \tag{58}$$

where

$$B'(\boldsymbol{W}', \overline{\boldsymbol{U}}, \boldsymbol{U}') \equiv B_1(\boldsymbol{W}', \overline{\boldsymbol{U}}, \boldsymbol{U}') - \left(\nabla \boldsymbol{w}', \boldsymbol{u}' \otimes \boldsymbol{u}'\right)_{\mathrm{Q}} + (\nabla^s \boldsymbol{w}', 2\nu'_T \nabla^s \boldsymbol{u}')_{\mathrm{Q}}. \tag{59}$$

This is the modeled small-scale equation which replaces (52). The large-scale equation, (51), remains the same, i.e., there is *no* modeling.

Remarks.

1. We shall refer to the term $\left(\nabla \boldsymbol{w}', \boldsymbol{u}' \otimes \boldsymbol{u}'\right)_{\mathrm{Q}}$ as the *small-scale Reynolds stress term* to distinguish it from $(\nabla \overline{\boldsymbol{w}}, \boldsymbol{u}' \otimes \boldsymbol{u}')_{\mathrm{Q}}$, the classical Reynolds stress term.
2. We have used the notation $\boldsymbol{R}'_S$ rather than $\boldsymbol{T}'_S$ to emphasize that we are modeling a missing effect whose origin is the small-scale Reynolds stress rather than the subgrid-scale stress.
3. By virtue that our modeling assumption involves the role of the small-scale Reynolds stress term, we might consider omitting it from (59). This engenders some computational simplifications which may facilitate the development of approximate analytical solutions to the small-scale equation. In any case, everything else is accounted for *exactly*, in particular, the classical Reynolds stress, cross-stress and Leonard stress (cf. Salvetti and Banarjee [34], Salvetti et al. [36], and Salvetti and Beux [35]).

6.4 Eddy viscosity models

We shall consider two candidate definitions of ν'_T. In both cases we shall estimate parameters by way of the Lilly analysis (see Sect. 4.1). However, this time we shall assume there are two relevant wave-number scales: $\bar{k}$, the resolution limit of the space $\overline{\mathcal{V}}$, and k', the resolution limit of the space $\mathcal{V} = \overline{\mathcal{V}} \oplus \mathcal{V}'$. The interpretation of $\bar{k}$ is assumed to be similar to before (see Sect. 4.1). Fig. 8 schematically contrasts the present situation with classical LES.

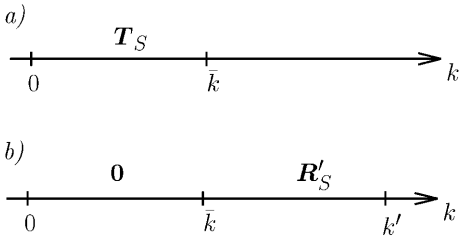

Fig. 8. a In classical LES, the subgrid-scale stress, $\boldsymbol{T}_S$, acts on all scales present, namely $k \in [0, \bar{k}]$. **b** In the multiscale method, the model of the effect of the small-scale Reynolds stress, $\boldsymbol{R}'_S$, acts only on the small scales, namely $k \in [\bar{k}, k']$

Note that in generalizing the Lilly analysis to the current situation, we will need to calculate spectral integrals over the interval $[\bar{k}, k']$ (see Fig. 9). Consequently we assume this interval lies entirely within the inertial subrange.

The assumed forms of ν'_T are:

$$\nu'_T = (C'_S \Delta')^2 \left|\nabla^s \boldsymbol{u}'\right| \tag{60}$$

and

$$\nu'_T = (C'_S \Delta')^2 \left|\nabla^s \overline{\boldsymbol{u}}\right|. \tag{61}$$

In the first case, ν'_T depends exclusively on small-scale velocity components. In the second case, ν'_T depends on the large-scale components. Intuitively, the first case may seem superior in that it is more consistent with the physical basis of the model. However, the second case offers some computational simplifications that make it worth considering too. Note that for (60), $\boldsymbol{R}'_S$ is completely desensitized to large scales, whereas for (61), $\boldsymbol{R}'_S$ is partially desensitized.

As before, $|\nabla^s \overline{\boldsymbol{u}}|$ is evaluated through (24) and (25); the small-scale counterpart is evaluated with (24) and

$$\tfrac{1}{2}\left|\nabla^s \boldsymbol{u}'\right|^2 = \int_{\bar{k}}^{k'} k^2 E(k)\, dk. \tag{62}$$

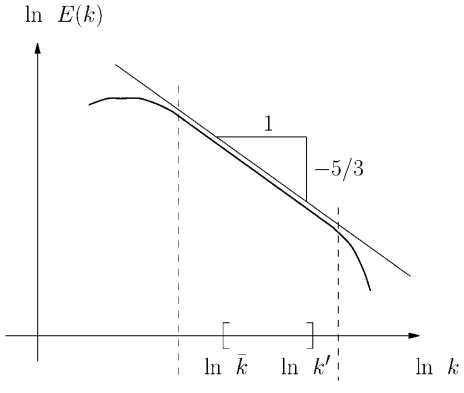

Fig. 9. Kolmogorov energy spectrum. The interval of small scales is assumed to lie within the inertial subrange

With this result in hand, calculations similar to (26) yield:

$$C'_S\Delta' = \left(\frac{2}{3\alpha}\right)^{3/4} \bar{k}^{-1}\,[(k'/\bar{k})^{4/3} - 1]^{-3/4} \tag{63}$$

$$C'_S\Delta' = \left(\frac{2}{3\alpha}\right)^{3/4} \bar{k}^{-1}\,[(k'/\bar{k})^{4/3} - 1]^{-1/2} \tag{64}$$

corresponding to (60) and (61), respectively. For a given discretization, from which $\bar{k}$ and k' can be determined, (63) and (64) determine $C'_S\Delta'$ for the two cases considered.

Remarks.

1. Note that fixing $\bar{k}$ in (63) and (64) implies that

$$k' \quad \uparrow \downarrow \quad \Leftrightarrow \qquad C'_S\Delta' \quad \downarrow \uparrow \tag{65}$$

for both cases, confirming the intuitively obvious result that the inclusion of more small scales reduces the size of $C'_S\Delta'$, and vice versa. If we select $\Delta' = \pi\bar{k}^{-1}$, as in Remark 1 of Sect. 4.1, we see from (63) and (64) that C'_S is just a function of the Kolmogorov constant, α, and the ratio $k'/\bar{k}$.

2. We can also reverse the argument and ask: For fixed $\bar{k}$ and $C'_S\Delta' = C_S\Delta$ (i.e., the value for the classical Smagorinsky model) what is k'? The answer to this question determines the size of $\mathcal{V}'$ compared to $\overline{\mathcal{V}}$. It turns out that for both (63) and (64),

$$k' = 2^{3/4}\bar{k} \;\approx\; 1.7\bar{k}. \tag{66}$$

Roughly speaking, the resolution limit needs to be almost twice as great. If we assume

$$k'/\bar{k} = \bar{h}/h' \tag{67}$$

(66) implies

$$h' = \bar{h}/2^{3/4} \;\approx\; 0.6\bar{h}, \tag{68}$$

which amounts to a finer mesh by almost a factor of two in each direction. This may seem daunting, but keep in mind that we can employ less refinement with a corresponding increase in the value of $C'_S\Delta'$ (by (63) and (64)). An even more attractive option may be the analytical determination of $\boldsymbol{U}'$ and its *a priori* elimination from the large-scale equation, that is, (51). For simple cases, this appears to be a real possibility (work in progress with F. Brezzi and A. Russo).

Note that for (66)–(68) we have, as before,

$$C'_S\Delta' = O(\bar{h}) \tag{69}$$

$$\nu'_T = O(\bar{h}^{4/3}). \tag{70}$$

However, keep in mind that $\boldsymbol{R}'_S$ only acts on the small scales.

3. The reason for considering (61), in which ν'_T is determined by $|\nabla^s\overline{\boldsymbol{u}}|$ rather than $\left|\nabla^s\boldsymbol{u}'\right|$, as in (60), is that, if we omit the small-scale Reynolds stress term, $\left(\nabla\boldsymbol{w}', \boldsymbol{u}'\otimes\boldsymbol{u}'\right)_{\mathrm{Q}}$, in the modeled small-scale equation, (58)–(59), it becomes linear in $\boldsymbol{U}'$, thus simplifying its numerical (and possibly, analytical) solution. In the numerical case we proceed as follows: Introducing a basis for $\mathcal{V}'$ such that

$$\boldsymbol{U}'(\boldsymbol{x}, t) = \sum_A N'_A(\boldsymbol{x}, t)\boldsymbol{U}'_A \tag{71}$$

$$\boldsymbol{U}'_A = \left\{\boldsymbol{u}'_A,\, p'_A\right\} \tag{72}$$

where N'_A are the basis functions and $\boldsymbol{U}'_A$ the corresponding nodal values, leads to a linear matrix problem:

$$\boldsymbol{K}\boldsymbol{U}' = -\boldsymbol{R} \tag{73}$$

$$\sum_B \boldsymbol{K}_{AB}\boldsymbol{U}'_B = -\boldsymbol{R}_A \tag{74}$$

so that

$$\boldsymbol{U}'_B = \sum_A \left(\boldsymbol{K}^{-1}\right)_{BA}(-\boldsymbol{R}_A) \tag{75}$$

$$\begin{aligned}\boldsymbol{U}'(\boldsymbol{x}, t) &= \sum_B N'_B(\boldsymbol{x}, t)\boldsymbol{U}'_B \\ &= -\sum_{A,B} N'_B(\boldsymbol{x}, t)(\boldsymbol{K}^{-1})_{BA}\boldsymbol{R}_A.\end{aligned} \tag{76}$$

For simplicity of exposition, we assumed an equal-order basis for $\boldsymbol{u}$ and p. In practice, this need not be the case. Note that the linear operator $\boldsymbol{K}$ depends on $\overline{\boldsymbol{U}}$.

4. In the case of (60), the fine small-scale equation becomes nonlinear through the dependence of ν'_T on $\left|\nabla^s\boldsymbol{u}'\right|$. In this case, nonlinear algebraic equations need to be solved to determine $\boldsymbol{U}'$.

6.5 Summary

For convenience, we summarize the main LES/variational multiscale equations here:

Large Scales.

$$B(\overline{\boldsymbol{W}}, \overline{\boldsymbol{U}}) + B_1(\overline{\boldsymbol{W}}, \overline{\boldsymbol{U}}, \boldsymbol{U}') = (\nabla\overline{\boldsymbol{w}}, \boldsymbol{u}'\otimes\boldsymbol{u}')_{\mathrm{Q}} + \left(\overline{\boldsymbol{W}}, \boldsymbol{F}\right) \tag{77}$$

Small Scales.

$$B_1(\boldsymbol{W}', \overline{\boldsymbol{U}}, \boldsymbol{U}') - (\nabla\boldsymbol{w}', \boldsymbol{u}'\otimes\boldsymbol{u}')_{\mathrm{Q}} = -\left[B(\boldsymbol{W}', \overline{\boldsymbol{U}} - \left(\boldsymbol{W}', \boldsymbol{F}\right)\right]. \tag{78}$$

Modeled Small Scales.

$$B'(\boldsymbol{W}', \overline{\boldsymbol{U}}, \boldsymbol{U}') = -\left[B(\boldsymbol{W}', \overline{\boldsymbol{U}}) - \left(\boldsymbol{W}', \boldsymbol{F}\right)\right] \tag{79}$$

where

$$\begin{aligned}B'(\boldsymbol{W}', \overline{\boldsymbol{U}}, \boldsymbol{U}') = {} & B_1(\boldsymbol{W}', \overline{\boldsymbol{U}}, \boldsymbol{U}') - \left(\nabla\boldsymbol{w}', \boldsymbol{u}'\otimes\boldsymbol{u}'\right)_{\mathrm{Q}} \\ & + (\nabla^s\boldsymbol{w}', 2\nu'_T\nabla^s\boldsymbol{u}')_{\mathrm{Q}}\end{aligned} \tag{80}$$

and

$$\nu'_T = (C'_S\Delta')^2\left|\nabla^s\boldsymbol{u}'\right| \tag{81}$$

or

$$\nu'_T = (C'_S \Delta')^2 \left|\nabla^s \overline{\boldsymbol{u}}\right| . \tag{82}$$

Modeled System.
A concise way of writing the combined system of (77) and (79) is

$$\overline{B}(\boldsymbol{W}, \boldsymbol{U}) = (\boldsymbol{W}, \boldsymbol{F}) \tag{83}$$

where

$$\overline{B}(\boldsymbol{W}, \boldsymbol{U}) \equiv B(\boldsymbol{W}, \boldsymbol{U}) + (\nabla^s \boldsymbol{w}', 2\nu'_T \nabla^s \boldsymbol{u}')_{\mathsf{Q}}. \tag{84}$$

Kinetic Energy Decay Inequality for the Modeled System.
This follows immediately from (83) with $\boldsymbol{W}$ replaced by $\boldsymbol{U}$:

$$\tfrac{1}{2}\left|\left|\boldsymbol{u}(T^-)\right|\right|^2_{\Omega} + 2\nu \left|\left|\nabla^s \boldsymbol{u}\right|\right|^2_{\mathsf{Q}} + \left|\left|(2\nu'_T)^{1/2} \nabla^s \boldsymbol{u}'\right|\right|^2_{\mathsf{Q}} \leq \tfrac{1}{2}\left|\left|\boldsymbol{u}(0^-)\right|\right|^2_{\Omega} + (\boldsymbol{u}, \boldsymbol{f})_{\mathsf{Q}} \tag{85}$$

which leads to

$$\tfrac{1}{2}\left|\left|\boldsymbol{u}(T^-)\right|\right|^2_{\Omega} + \nu \left|\left|\nabla^s \boldsymbol{u}\right|\right|^2_{\mathsf{Q}} + \left|\left|(2\nu'_T)^{1/2} \nabla^s \boldsymbol{u}'\right|\right|^2_{\mathsf{Q}} \leq \tfrac{1}{2}\left|\left|\boldsymbol{u}(0^-)\right|\right|^2_{\Omega} + \frac{C_{\Omega}}{4\nu} ||\boldsymbol{f}||^2_{\mathsf{Q}} . \tag{86}$$

Remarks.

1. Note, if $\overline{\boldsymbol{U}}$ is an exact solution of the Navier–Stokes equations, then

$$B(\boldsymbol{W}, \overline{\boldsymbol{U}}) = (\boldsymbol{W}, \boldsymbol{F}) \qquad \forall \boldsymbol{W} \in \mathcal{V}. \tag{87}$$

In particular,

$$B(\boldsymbol{W}', \overline{\boldsymbol{U}}) = (\boldsymbol{W}', \boldsymbol{F}) \qquad \forall \boldsymbol{W}' \in \mathcal{V}'. \tag{88}$$

Consequently, for both the exact and the modeled small-scale equations (i.e., (78) and (79), respectively), it follows that $\boldsymbol{U}' = \boldsymbol{0}$. We also have from (87) that

$$B(\overline{\boldsymbol{W}}, \overline{\boldsymbol{U}}) = (\overline{\boldsymbol{W}}, \boldsymbol{F}) \qquad \forall \overline{\boldsymbol{W}} \in \overline{\mathcal{V}}. \tag{89}$$

These results verify that (77) is identically satisfied. This means the equation governing the large scales retains its *consistency*, or residual structure, despite the modeling of small scales, in contrast to the classical LES case described in Sect. 4.

2. By virtue of the fact that $\boldsymbol{U}' = \{\boldsymbol{u}', p'\} \in \mathcal{V}' \subset \mathcal{V}$, $\boldsymbol{u}' = \boldsymbol{0}$ on P. Furthermore, the small-scales equations (either (78) or (79)) imply $\nabla \cdot \boldsymbol{u}' = 0$ on Q. From this we may conclude that $\boldsymbol{u}'$ attains the correct asymptotic structure near walls by the usual argument. In particular, the [1,2] component of $\boldsymbol{u}' \otimes \boldsymbol{u}'$ in (77) behaves like x_2^3, where x_1 is the streamwise direction and x_2 is the direction normal to the wall.

3. Assuming, for expositional simplicity, equal-order interpolation of the large scales, solution of (77) proceeds by expanding

$$\overline{\boldsymbol{U}}(\boldsymbol{x}, t) = \sum_B \overline{N}_B(\boldsymbol{x}, t) \overline{\boldsymbol{U}}_B \tag{90}$$

where

$$\overline{\boldsymbol{U}}_B = \left\{\overline{\boldsymbol{u}}_B, \overline{p}_B\right\} \tag{91}$$

and

$$\overline{\boldsymbol{W}}(\boldsymbol{x}, t) = \sum_A \overline{N}_A(\boldsymbol{x}, t) \overline{\boldsymbol{W}}_A \tag{92}$$

$$\overline{\boldsymbol{W}}_A = \left\{\overline{\boldsymbol{w}}_A, \bar{q}_A\right\} . \tag{93}$$

Substituting into (77) yields nonlinear equations for the $\overline{\boldsymbol{U}}_B$'s. $\boldsymbol{U}'$ is determined by the procedures described in Remarks 3 and 4 in Sect. 6.4.

4. Our approach has both similarities to, and differences with, the work of Temam and colleagues. The similarities are that both approaches invoke scale separation from the outset and both employ projected forms of the Navier–Stokes equations, rather than the filtered versions used in LES. The salient differences are as follows: In the earlier work of the Temam group (see Dubois et al. [9] for a representative exposition):

(i) In the equation governing large-scales, the classical Reynolds stress term is neglected.
(ii) In the equation governing small scales, the only term acting on small scales which is retained is the Stokes operator term. In particular, the cross-stress, time-derivative and small-scale Reynolds stress terms are neglected.

These assumptions are strong ones and can be shown to limit the applicability of the approach to discretizations which are only somewhat coarser than required for DNS. Otherwise excessive dissipation is encountered. This may be contrasted with our approach in which all these terms are retained, except that the effect of the small-scale Reynolds stress term is modeled. Obviously, we assume it is important to retain the terms omitted in the Temam's group earlier work.

In more recent work (see Dubois et al. [10]), Temam and co-workers retain all the terms omitted in their previous work and adopt an adaptive strategy in space and time to resolve small-scale behavior. In our opinion, this is a DNS approach, although Dubois et al. [10] characterize it as somewhere between LES and DNS. Our approach is similar, except for the modeling of the small-scale Reynolds stress term. We thus feel it is appropriate to characterize our formulation as LES, or at least closer to LES than that of Dubois et al. [10].

5. Farge et al. [11] present a very interesting analysis of two-dimensional turbulence based on an adaptive wavelet decomposition of the vorticity into coherent, non-Gaussian structures, and an incoherent, Gaussian background. The efficiency of the wavelet representation is illustrated in a DNS computation of a mixing layer in which the time evolution of the coherent part only involves 8% of the wavelet coefficients. The remaining coefficients, associated with the incoherent part, are simply discarded at each time step. In order to maximize data compression, the velocity-vorticity form of the Navier–Stokes equations is employed in preference to the velocity-pressure form.

The wavelet decomposition at each time step is an example of *a priori* scale separation, as advocated in the present work. However, when Farge et al. [11] discuss modeling they do so in the context of the filtered form of the equations, as in classical LES, and are faced with the problem of representing the subgrid-scale stress $\boldsymbol{T}$. They propose the following

possibilities: (i) The Smagorinsky model; (ii) a dynamic generalization in which the eddy viscosity ν_T is estimated in terms of the enstrophy fluxes in wavelet space, such that when energy flows from large to small scales ν_T will be positive and vice versa (i.e., backscatter); and (iii) the subgrid-scale stress $\boldsymbol{T}$ modeled as a Gaussian forcing term proportional to the variance of the incoherent parts of the vorticity and velocity. In modeling $\boldsymbol{T}$ in these ways it seems inevitable that at least some of the shortcomings associated with the use of the filtered equations will eventually be encountered. For example, $\boldsymbol{T}$ may act too strongly on the coherent (i.e., resolved) structures, and there seems no *a priori* control of kinetic energy if backscatter occurs. However, it would seem possible to reformulate the numerical procedure in terms of the variational multiscale method, associating coherent structures with the space $\overline{\mathcal{V}}$ and the incoherent background with $\mathcal{V}'$. In this way some difficulties might be circumvented, but the efficiency of the method might also be compromised.

6. In Appendix A we present a sketch of a semi-discrete version of the theory which has similar properties to the space-time formulation.

7 Computational issues

In the case of finite element discretizations, the numerical stability of $\overline{\boldsymbol{u}}$, $\overline{p}$, $\boldsymbol{u}'$ and p' require some attention. The following remarks may be helpful.

Remarks.

1. The eddy viscosity term should be sufficient to stabilize $\boldsymbol{u}'$.

2. The $\boldsymbol{u}'$ will provide some stability for $\overline{p}$ and $\overline{\boldsymbol{u}}$, but possibly not enough, unless a special $\boldsymbol{u}'$ is developed. We may need to consider additional *stabilization* of $\overline{\boldsymbol{u}}$, $\overline{p}$ by way of say the *Galerkin/least-squares procedure*, for example. Let $\mathcal{N}(\overline{\boldsymbol{U}}) = \boldsymbol{f}$, where

$$\mathcal{N}(\overline{\boldsymbol{U}}) = \frac{\partial \overline{\boldsymbol{u}}}{\partial t} + \nabla\cdot(\overline{\boldsymbol{u}}\otimes\overline{\boldsymbol{u}}) + \nabla\overline{p} - \nu\Delta\overline{\boldsymbol{u}} \tag{94}$$

The additional term to be added to (77), or equivalently (83), is

$$\int_{\widetilde{\mathrm{Q}}} \left(\frac{\partial \overline{\boldsymbol{w}}}{\partial t} + \nabla\cdot(\overline{\boldsymbol{w}}\otimes\overline{\boldsymbol{u}}) + \nabla\overline{q} - \nu\Delta\overline{\boldsymbol{w}} \right) \times \boldsymbol{\tau}\left(\mathcal{N}(\overline{\boldsymbol{U}}) - \boldsymbol{f}\right)\, d\mathrm{Q} \tag{95}$$

where $\widetilde{\mathrm{Q}}$ denotes the interiors of elements.

Notes.

(i) In (95),

$$(\nabla\cdot(\overline{\boldsymbol{w}}\otimes\overline{\boldsymbol{u}}))_i = \frac{\partial}{\partial x_j}\left(\overline{w}_i\overline{u}_j\right). \tag{96}$$

(ii) $\boldsymbol{\tau}$ is symmetric and positive semi-definite. See, for example, Franca et al. [12] and Taylor et al. [38]. In the present case, $\boldsymbol{\tau}$ and/or ν_T' may need to be retuned for turbulence applications to produce the desired energy spectrum (see Remark 2, Sect. 5).

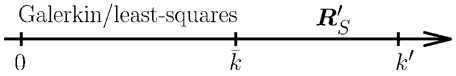

Fig. 10. Scale separation of stabilizing mechanisms

(iii) The inclusion of a Galerkin/least-squares term will modify the kinetic energy decay inequality (86) as follows:

$$\begin{aligned}\tfrac{1}{2}\left|\left|\boldsymbol{u}(T^-)\right|\right|_{\Omega}^2 + \nu\left|\left|\nabla^s\boldsymbol{u}\right|\right|_{\mathrm{Q}}^2 + \left|\left|(2\nu_T')^{1/2}\nabla^s\boldsymbol{u}'\right|\right|_{\mathrm{Q}}^2 \\ + \tfrac{1}{2}\left|\left|\boldsymbol{\tau}^{1/2}\mathcal{N}(\overline{\boldsymbol{U}})\right|\right|_{\widetilde{\mathrm{Q}}}^2 \le \tfrac{1}{2}\left|\left|\boldsymbol{u}(0^-)\right|\right|_{\Omega}^2 \\ + \frac{C_{\Omega}}{4\nu}\left|\left|\boldsymbol{f}\right|\right|_{\mathrm{Q}}^2 + \tfrac{1}{2}\left|\left|\boldsymbol{\tau}^{1/2}\boldsymbol{f}\right|\right|_{\widetilde{\mathrm{Q}}}^2\end{aligned} \tag{97}$$

Note that in this case there is scale separation between dissipative mechanisms. See Fig. 10. Despite the prohibition against algorithmic dissipation in LES applications, (95) retains the residual structure of the equations and may not seriously degrade the behavior of the model. This conjecture, of course, would require testing. Based on the results of Jansen et al. [25], if piecewise linears were used for $\overline{\boldsymbol{u}}$, then the Laplacian terms in (94) and (95) would require variational reconstruction. If quadratics, or higher-order, interpolations are employed, this may not be necessary.

3. The stability of p' is the final consideration. Since we do not want to add any additional dissipative mechanism, p' is subject to an *inf-sup* condition (see Brezzi and Fortin [1] and Quarteroni and Valli [33]). A simple possibility is to use classical bubbles for $\boldsymbol{u}'$ and p'=0. Some stable elements for the Stokes problem are constructed this way. Note that $\boldsymbol{u}'$ is incompressible in the mean with respect to each element. If hierarchical polynomial refinement is considered, the inf-sup condition needs to be addressed on a case-by-case basis.

4. Local conservation is often considered an attribute for schemes used for LES applications. Local conservation of mass and momentum can be attained by going from a continuous Galerkin formulation on each space-time slab to a fully discontinuous Galerkin formulation (i.e., with respect to both space and time). Local conservative quantities can also be constructed within the continuous Galerkin method by a post-processing procedure (see, e.g., Hughes [19], p.107). Furthermore, there are some locally mass conserving elements within the Galerkin formulation (see Hughes [19]).

8 Conclusions

In this paper we have developed a variational multiscale approach to Large Eddy Simulation, suitable for finite element discretizations as well as other discretization approaches. The variational multiscale approach is a technique for the *a priori* separation of scales. This is followed by modeling the effect of the "small-scale Reynolds stress." Our approach may be contrasted with classical LES in which modeling of the

subgrid-scale stress in the filtered equations is performed first, and scale separation is accomplished *a posteriori* by, for example, the dynamic modeling procedure.

Criticisms lodged against the classical LES/Smagorinsky model are addressed in the present approach. Specifically, even with a positive, constant-coefficient, eddy viscosity term, the present approach:

1. Yields the correct asymptotic behavior at walls for the classical Reynolds stress, cross-stress, Leonard stress and, consequently, the subgrid-scale stress. In particular, no modeling of these terms is performed.

2. Reduces dissipation in the presence of mean shear.

3. Accommodates backscatter, whereas at the same time correct kinetic energy decay inequalities are *a priori* satisfied for the total solution $\boldsymbol{u} = \overline{\boldsymbol{u}} + \boldsymbol{u}'$, guaranteeing stability. We believe this is the natural way to simulate backscatter.

4. Ameliorates damping of resolved structures since the eddy viscosity term acts only on fluctuations.

Furthermore, the present approach de-emphasizes the role of the Smagorinsky constant in producing dissipation, but accentuates dissipation effects associated with fluctuations. Consequently, a single value of the constant, selected, say, in the traditional way, by modeling the decay of homogeneous isotropic turbulence, may behave in a satisfactory manner for a variety of complex flows.

In addition, the variational equation governing large scales, which is unmodeled in our approach, is identically satisfied by all exact solutions of the Navier–Stokes equations. This is often referred to as the "consistency condition" and is a key condition for obtaining error estimates. This may be contrasted with the classical LES/constant-coefficient Smagorinsky model case which does not possess this property.

On the other hand, we note that the eddy viscosity models considered herein are very simple, perhaps too simple. It would appear worthwhile to develop generalizations accounting for unstructured, high-aspect ratio meshing, as well as boundary layer behavior. Dynamic modeling may also provide an avenue for improvement.

We would like to take the opportunity to summarize the main tenets of the approach proposed herein in contradistinction to classical LES. We advocate:

(i) Variational projection in preference to filtering. This obviates the closure problem and with it the necessity of modeling the subgrid-scale stress. In addition, complex issues associated with filtering and inhomogeneous wall-bounded flows are also eliminated.

(ii) *A priori* scale separation in preference to *a posteriori* scale separation. This facilitates modeling restricted to unresolved, high-wave number phenomena rather than all wave numbers as in classical LES.

(iii) Modeling confined to the small-scale equation in preference to modeling within the large-scale equation. This means that the large-scale equation is unmodeled and is consistent in the weighted residual sense, in contrast to the modeled filtered equations.

Obviously, at this juncture, this is all a very speculative business, since testing and validation studies have not been performed. However, we are, in particular, hopeful that the ideas described herein may lead to improved versions of finite element programs currently used for LES (e.g., see Chalot et al. [7], "Spectrum" [6, 18], Jansen [23, 24]). Furthermore, we hope that the present formulation of LES will enable approximation theorists to more readily bring their talents to bear on the subject. Finally, we hope that this work will also provide some amusement and stimulation to the turbulence community.

Acknowledgements. The senior author would like to thank: P.-L. Lions and A. Quarteroni for inviting me to contribute this paper; P. Moin for patiently trying to educate me about turbulence and LES; F. Brezzi, D. Marini and A. Russo for clarifying many mathematical concepts; M.V. Salvetti and F. Beux for helpful discussions; the Scuola Normale Superiore, Pisa, and the Associazione Amici della Scuola Normale Superiore, for making possible my visit as the Cattedra Galileiana, and, in particular, G. Da Prato, C. Gulminelli and the Director of the Scuola Normale, F. Bassani.

Appendix A. Semi-discrete formulation

In this appendix we illustrate the ideas in terms of a more traditional semi-discrete formulation in which a midpoint rule algorithm is used for time discretization. Let $\boldsymbol{u}_n$ and p_n represent the algorithmic solution at time t_n. The time step is denoted $\Delta t = t_{n+1} - t_n$. It proves convenient to employ the jump and mean value operators, viz.,

$$[\boldsymbol{u}] = \boldsymbol{u}_{n+1} - \boldsymbol{u}_n \tag{A.1}$$

$$\langle \boldsymbol{u} \rangle = \tfrac{1}{2} (\boldsymbol{u}_{n+1} + \boldsymbol{u}_n) . \tag{A.2}$$

The algorithm is an approximation to the semi-discrete variational formulation, given as follows:

$$\left(\boldsymbol{w}, \frac{\partial \boldsymbol{u}}{\partial t} \right)_{\Omega} - (\nabla \boldsymbol{w}, \boldsymbol{u} \otimes \boldsymbol{u})_{\Omega} + (q, \nabla \cdot \boldsymbol{u})_{\Omega}$$
$$- (\nabla \cdot \boldsymbol{w}, p)_{\Omega} + \left(\nabla^s \boldsymbol{w}, 2\nu \nabla^s \boldsymbol{u} \right)_{\Omega} = (\boldsymbol{w}, \boldsymbol{f})_{\Omega} \tag{A.3}$$

Midpoint rule

$$\frac{1}{\Delta t} (\boldsymbol{w}, [\boldsymbol{u}])_{\Omega} - (\nabla \boldsymbol{w}, \langle \boldsymbol{u} \rangle \otimes \langle \boldsymbol{u} \rangle)_{\Omega} + (q, \nabla \cdot \langle \boldsymbol{u} \rangle)_{\Omega}$$
$$- (\nabla \cdot \boldsymbol{w}, \langle p \rangle)_{\Omega} + \left(\nabla^s \boldsymbol{w}, 2\nu \nabla^s \langle \boldsymbol{u} \rangle \right)_{\Omega} = (\boldsymbol{w}, \langle \boldsymbol{f} \rangle)_{\Omega} \tag{A.4}$$

The kinetic energy evolution law immediately follows from (A.4) by replacing $\boldsymbol{w}$ with $\langle \boldsymbol{u} \rangle$ and q with $\langle p \rangle$, i.e.,

$$\tfrac{1}{2} ||\boldsymbol{u}_{n+1}||^2_{\Omega} + 2\nu \Delta t \left|\left| \nabla^s \langle \boldsymbol{u} \rangle \right|\right|^2_{\Omega} = \tfrac{1}{2} ||\boldsymbol{u}_n||^2_{\Omega} + \Delta t \, (\langle \boldsymbol{u} \rangle, \langle \boldsymbol{f} \rangle)_{\Omega} . \tag{A.5}$$

We also have

$$\tfrac{1}{2} ||\boldsymbol{u}_{n+1}||^2_{\Omega} + \nu \Delta t \left|\left| \nabla^s \langle \boldsymbol{u} \rangle \right|\right|^2_{\Omega} \leq \tfrac{1}{2} ||\boldsymbol{u}_n||^2_{\Omega} + \frac{C_{\Omega} \Delta t}{4\nu} ||\langle \boldsymbol{f} \rangle||^2_{\Omega} \tag{A.6}$$

where C_{Ω} is defined by (38).

The multiscale procedure is developed in analogous fashion to the space-time case (see Sect. 6). Let

$$\boldsymbol{u}_n = \overline{\boldsymbol{u}}_n + \boldsymbol{u}'_n \tag{A.7}$$

$$p_n = \overline{p}_n + p'_n \tag{A.8}$$

$$\boldsymbol{w} = \overline{\boldsymbol{w}} + \boldsymbol{w}' \tag{A.9}$$

$$q = \overline{q} + q' . \tag{A.10}$$

These are substituted into (A.4) resulting in equations governing large and small scales, as before. We leave the details, which are straightforward, to the interested reader. Modeling also follows the ideas developed previously, namely, to the left-hand side of (A.4) we add the term

$$\left(\nabla^s \boldsymbol{w}', 2\nu'_T \nabla^s \langle \boldsymbol{u}' \rangle\right)_\Omega . \tag{A.11}$$

This amounts to adding viscous dissipation to the small scales equation. The modification to the kinetic energy identity, (A.5), is

$$\begin{aligned} \tfrac{1}{2}\,||\boldsymbol{u}_{n+1}||^2_\Omega + 2\nu\Delta t\,\left|\left|\nabla^s\langle\boldsymbol{u}\rangle\right|\right|^2_\Omega + \Delta t\,\left|\left|(2\nu'_T)^{1/2}\nabla^s\langle\boldsymbol{u}'\rangle\right|\right|^2_\Omega \\ = \tfrac{1}{2}\,||\boldsymbol{u}_n||^2_\Omega + \Delta t\,(\langle\boldsymbol{u}\rangle, \langle\boldsymbol{f}\rangle)_\Omega \end{aligned} \tag{A.12}$$

from which follows:

$$\begin{aligned} \tfrac{1}{2}\,||\boldsymbol{u}_{n+1}||^2_\Omega + \nu\Delta t\,\left|\left|\nabla^s\langle\boldsymbol{u}\rangle\right|\right|^2_\Omega + \Delta t\,\left|\left|(2\nu'_T)^{1/2}\nabla^s\langle\boldsymbol{u}'\rangle\right|\right|^2_\Omega \\ \leq \tfrac{1}{2}\,||\boldsymbol{u}_n||^2_\Omega + \frac{C_\Omega \Delta t}{4\nu}\,||\langle\boldsymbol{f}\rangle||^2_\Omega \end{aligned} \tag{A.13}$$

Remark. As remarked previously, the term $(\nabla\langle\boldsymbol{w}\rangle, \langle\boldsymbol{u}\rangle\otimes\langle\boldsymbol{u}\rangle)_\Omega$ may need to be altered in the discrete case in order to achieve

$$(\nabla\langle\boldsymbol{u}\rangle, \langle\boldsymbol{u}\rangle\otimes\langle\boldsymbol{u}\rangle)_\Omega = 0. \tag{A.14}$$

See Quarteroni and Valli [33], p. 435.

References

1. Brezzi, F., Fortin, M. Mixed and Hybrid Finite Element Methods. Berlin: Springer-Verlag 1991
2. Brezzi, F., Franca, L.P., Hughes, T.J.R., Russo, A. $b = \int g$. Computer Meth. Appl. Mech. Eng. 145, 329–339 (1997)
3. Brezzi, F., Houston, P., Marini, D., Süli, E. Modeling Subgrid Viscosity for Advection-Diffusion Problems. Preprint, 1999
4. Brezzi, F., Hughes, T.J.R., Marini, D., Russo, A., Süli, E. A Priori Error Analysis of a Finite Element Method with Residual-Free Bubbles for Advected-Dominated Equations. SIAM J. Numer. Anal. 36, 1933–1948 (1999)
5. Brezzi, F., Marini, D., Süli, E. Residual-Free Bubbles for Advection-Diffusion Problems: The General Error Analysis. Preprint, 1999
6. Centric Engineering Systems, Inc. Spectrum^{TM} Theory Manual 1994
7. Chalot, F., Marquez, B., Ravachal, M., Ducros, F., Nicoud, F., Poinsot, T. A Consistent Finite Element Approach to Large Eddy Simulation. Technical Report 98-2652, 29th AIAA Fluid Dynamics Conference, Albuquerque, New Mexico, June 15-18, 1998
8. David, E. Modélisation des Ecoulement Compressibles et Hypersoniques. Une Approche Instationnaire. Ph. D. thesis, Institut National Polytechnique de Grenoble, 1993
9. Dubois, T., Jauberteau, F., Temam, R. Solution of the Incompressible Navier-Stokes Equations by the Nonlinear Galerkin Method. J. Sci. Computing 8, 167–194 (1993)
10. Dubois, T., Jauberteau, F., Temam, R. Incremental Unknowns, Multilevel Methods and the Numerical Simulation of Turbulence. Comp. Meth. Appl Mech. Eng. 159, 123–189 (1998)
11. Farge, M., Schneider, K, Kevlahan, N. Non-Gaussianity and Coherent Vortex Simulation for Two-Dimensional Turbulence using an Adaptive Wavelet Basis. Phys. Fluids 11, 2187–2201 (1999)
12. Franca, L.P., Frey, S.L., Hughes, T.J.R. Stabilized Finite Element Methods: I. Application to the Advection-Diffusion Model. Comp. Meth. Appl. Mech. Eng. 95, 253–276 (1992)
13. Franca, L.P., (Ed). Special Issue on "Advances in Stabilized Methods in Computational Mechanics". Comp. Meth. Appl. Mech. Eng. 166, (November 1998)
14. Galdi, G.P., Layton, W.J: Approximation of the Larger Eddies in Fluid Motion II: A Model for Space-Filtered Flow. To appear in Mathematical Models and Methods in Applied Sciences 1999
15. Germano, M., Piomelli, U., Moin, P., Cabot, W.H. A Dynamic Subgrid-Scale Model. Phys. Fluids A, Fluid Dynamics 3, 1760–1765 (1991)
16. Ghosal, S., Moin, P. The Basic Equations for the Large-Eddy Simulation of Turbulent Flows in Complex-Geometry. J. Comp. Phys. 118, 24–37 (1995)
17. Guermond, J.-L. Subgrid Stabilization of Galerkin Approximations of Monotone Operators. In: Proceedings of the European Science Foundation Conference on Applied Mathematics for Industrial Flow Problems (AMIF) San Feliu de Guixols (Costa Brava), Spain, 1998
18. Holmes, B.S., Dias, J.B., Jaroux, B.A., Sassa, T., Ban, Y. Predicting the Wind Noise from the Pantograph Cover of a Train. Int. J. Numer. Meth. Fluids 24, 1307–1319 (1997)
19. Hughes, T.J.R. The Finite Element Method: Linear Static and Dynamic Finite Element Analysis. Englewood Cliffs: Prentice-Hall 1987
20. Hughes, T.J.R. Multiscale Phenomena: Green's functions, the Dirichlet-to-Neumann Formulation, Subgrid Scale Models, Bubbles and the Origin of Stabilized Methods. Comp. Meth. Appl. Mech. Eng. 127, 387–401 (1995)
21. Hughes, T.J.R., G.R. Feijóo, Mazzei, L., Quincy, J.-B. The Variational Multiscale Method – A Paradigm for Computational Mechanics. Comp. Meth. Appl. Mech. Eng. 166, 3–24 (1998)
22. Hughes, T.J.R., Stewart, J.R. A Space-Time Formulation for Multiscale Phenomena. J. Comp. Appl. Math. 74, 217–229 (1996)
23. Jansen, K.E. Large-Eddy Simulations of Flow around a NACA 4412 Airfoil using Unstructured Grids. CTR Annual Research Briefs, pp. 225–232, Center for Turbulence Research, Stanford University/NASA Ames Research Center, 1996
24. Jansen, K.E: Large-Eddy Simulation using Unstructured Grids. In: Liu, C., Liu, Z. (Eds.) Advances in DNS/LES. pp. 117–128. Columbus: Greyden 1997
25. Jansen, K.E., Whiting, C., Collis, S., Shakib, F. A Better Consistency for Low-Order Stabilized Finite Element Methods. To appear in Comp. Meth. Appl. Mech. Eng. 174, 153–170 (1999)
26. John, V., Layton, W.J. Approximation of the Larger Eddies in Fluid Motion, I.: Direct simulation for the Stokes Problem. Preprint, 1998
27. Layton, W.J. A Nonlinear Subgrid-Scale Model for Incompressible Viscous Flow Problems. SIAM J. Sci. Computing 17, 347–357 (1996)
28. Lilly, D.K. On the Application of the Eddy Viscosity Concept in the Inertial Subrange of Turbulence. NCAR Manuscript 123, Boulder, Colorado, 1966
29. Lilly, D.K. The Representation of Small-Scale Turbulence in Numerical Simulation Experiments. In Proceedings of the IBM Scientific Computing Symposium on Environmental Sciences Yorktown Heights, New York, 1967
30. Lilly, D.K. The Length Scale for Subgrid-Scale Parametrization with Anisotropic Resolution. Center for Turbulence Research, Stanford University/NASA Ames Research Center, 1988. CTR Annual Research Briefs, pp. 3–9
31. Moin, P., Squire, K., Cabot, W.H., Lee, S. A Dynamic Subgrid-Scale Model for Compressible Turbulence and Scalar Transport. CTR Manuscript 124, Center for Turbulence Research, Stanford University/NASA Ames Research Center, March 1991
32. Piomelli, U. Large Eddy Simulation: Present State and Future Directions. Technical Report 98-0534, AIAA, 1998
33. Quarteroni, A., Valli, A. Numerical Approximation of Partial Differential Equations. Berlin: Springer-Verlag 1994
34. Salvetti, M.V., Banarjee, S. A Priori Tests of a New Dynamic Subgrid-Scale Model for Finite Difference Large Eddy Simulations. Phys. Fluids 7, 2831–2847 (1995)
35. Salvetti, M.V., Beux, F. The Effect of the Numerical Scheme on the Subgrid Scale Term in Large Eddy Simulation. Phys. Fluids 10, 3020–3022 (1998)
36. Salvetti, M.V., Zang, Y., Street, R.L., Banarjee, S. Large Eddy Simulation of Free-Surface Decaying Turbulence with Dynamic Subgrid-Scale Models. Phys. Fluids 9, 2405–2419 (1997)
37. Smagorinsky, J. General Circulation Experiments with the Primitive Equations, I: The Basic Experiment. Month. Weath. Rev. 91, 99–164 (1963)
38. Taylor, C.A., Hughes, T.J.R., Zarins, C.K. Finite Element Modeling of Blood Flow in Arteries. Comp. Meth. Appl. Mech. Eng. 158, 155–196 (1998)
39. Temam, R. Navier–Stokes Equations. Theory and Numerical Analysis. 3rd Edition. Amsterdam: North-Holland 1984